Strange Baryon Production in Heavy Ion Collisions

by

A. Capella, A. Kaidalov*, A. Kouider Akil, C. Merino, J. Tran Thanh Van

Laboratoire de Physique Théorique et Hautes Energies **
Université de Paris XI, bâtiment 211, 91405 Orsay Cedex, France

Abstract

The rapidity distribution of Λ and $\bar{\Lambda}$ produced in nucleus-nucleus collisions at CERN energies is studied in the framework of an independent string model - with quark-antiquark as well as diquark-antidiquark pairs in the nucleon sea. It is shown that, besides the Λ-$\bar{\Lambda}$ pair production resulting from the fragmentation of sea diquarks, final state interactions of co-moving secondaries $\pi + N \to K + \Lambda$ and $\pi + \bar{N} \to K + \bar{\Lambda}$ are needed in order to reproduce the data. Predictions for *Pb-Pb* collisions are presented.

LPTHE Orsay 95-41

June 1995

* Present address : ITEP, B. Cheremushkinskaya ulitsa 25, 117 259 Moscow, Russia

** Laboratoire associé au Centre National de la Recherche Scientifique - URA D0063

1. Introduction

A substantial increase in the ratio of strange over non-strange particles between proton-proton and central nucleus-nucleus collisions has been observed experimentally both at CERN and AGS [1]. Such an increase was expected as a consequence of quark gluon plasma (QGP) formation due to an increase of the strange quark production rate in the deconfined phase [2]. However, as in the case of other possible signals of QGP, one has to check whether such a phenomenon is typical of a central nucleus-nucleus collision or, on the contrary, it is already present in proton-nucleus interactions *. Unfortunately, the experimental situation is not conclusive. While in the data from the NA35 collaboration strangeness is enhanced between pp and pS, the effect is not seen when taking an average over three different nuclear targets [4]. However, two other experimental facts indicate that strangeness enhancement is not only present in central nucleus-nucleus collisions. Indeed in pp collisions, the ratio K/π increases both with increasing energy and with increasing multiplicity [5]. Also the ratio $\bar{\Lambda}/\bar{p}$ in pp collisions increases from 0.26 at $\sqrt{s} = 20$ GeV [6] to 0.39 at $\sqrt{s} = 1\ 800$ GeV [7]. Furthermore, results from the NA36 collaboration [8] show a large strangeness enhancement between peripheral and average nucleus-nucleus collisions.

Actually, it has been emphasized [9-11] that strangeness enhancement is expected to occur in independent string models such as the Dual Parton Model (DPM) [9] and the Quark Gluon String Model (QGSM) [12]. Indeed, the average number

* For instance, in the case of J/ψ suppression, R. Salmeron, followed by many other authors, has shown that the effect could be explained by extrapolation of the corresponding hadron-nucleus data [3].

of collisions per participant nucleon increases between pp and pA as well as between pA and central AB collisions. The resulting extra particles are produced in the fragmentation of strings involving sea constituents at their ends. Since strange sea quarks are present in the nucleon sea, the ratio of strange over non-strange secondaries will also increase. The value of this increase depends on the ratio

$$S = \frac{2(s + \bar{s})}{u + d + \bar{u} + \bar{d}}$$

in the nucleon sea. We shall use a value of S in the range 0.4 to 0.5, consistent both with strangeness suppression in string fragmentation at the highest available energies [7] and with conventional parton distributions for DIS [13]. In order to explain the observed enhancement of Λ and $\bar{\Lambda}$, two approaches have been proposed. In DPM, diquark-antidiquark pairs have been introduced in the nucleon sea - with the same ratio, relative to quark-antiquark pairs, as in the string breaking process [10, 11]. The second approach is string fusion [14, 15]. However, both mechanisms have a common caveat, namely, they lead to the same increase in absolute value of strange baryons and antibaryons - while experimentally the excess of Λ's is much larger than that of $\bar{\Lambda}$'s.

In the present work we solve this problem by introducing final state interactions of co-moving pions and nucleons which increase the number of produced Λ's via the binary interactions $\pi + N \rightarrow K + \Lambda$ ($K^* + \Lambda$, ...). This is a fundamental mechanism in hadron gas models [2] and has been incorporated into some Monte Carlo codes [12, 15, 16]. Clearly, such an interaction is very efficient in producing Λ's - since the density of both pions and nucleons is high as compared to that of Λ's. Actually, it was shown in Ref. [11], that using the experimentally measured pion and nucleon densities in central SS collisions, together with the cross-section

of the above reaction (which is about 1.5 mb at the maximum near threshold), one precisely obtains the missing number of Λ's. Obviously, the conjugate reaction $\pi + \bar{N} \to K + \bar{\Lambda}$ $(K^* + \bar{\Lambda})$ will also produce some extra $\bar{\Lambda}$ but the absolute yield is much smaller than the one of Λ's due to the smallness of the $\bar{N}$ density as compared to that of N's.

In this paper we compute, in the framework described above, the rapidity distributions of Λ and $\bar{\Lambda}$ in SS and Pb-Pb collisions. A substantial increase of the ratios Λ/π^- and $\bar{\Lambda}/\pi^-$ (70 % and 50 %, respectively) is predicted between SS and Pb-Pb.

Extra evidence for the necessity of a final state interaction is obtained from baryon stopping. The rapidity distribution of proton minus antiproton in central SS collisions, computed in independent string models, has a dip at $y^* \sim 0$ which is much more pronounced that the one observed experimentally [17] - while the corresponding distributions both in pp and in peripheral SS collisions are well reproduced. In other words, the stopping power in the model is too small as compared to experiment and rescattering of the produced baryon is required in order to increase it [12] [15].

The plan of the paper is as follows : in Section 2 we give the general formulae of DPM for nucleus-nucleus collisions in the presence of diquark-antidiquark pairs in the nucleon sea and compute the rapidity distributions of Λ and $\bar{\Lambda}$ in pp and SS collisions without final state interactions. In Section 3, we introduce the final state interactions and give the modified Λ and $\bar{\Lambda}$ rapidity distributions in SS collisions as well as the model predictions for Pb-Pb collisions. The rapidity distribution of pions and protons in pp, SS and Pb-Pb collisions are also given. A list of

average multiplicities for pions, kaons, baryons and antibaryons without and with final state interactions is given in Table 1. Section 4 contains some final remarks and conclusions. In Appendix 1 we give the momentum distribution functions and fragmentation functions used in this work, as well as the formulae for the hadronic spectra of the individual strings.

2. The Model

In DPM and QGSM, the dominant contribution to multiparticle production in pp collisions is a two string production - the two strings being stretched between the valence diquark of a proton and a valence quark of the other proton, and vice-versa. In fact, in this paper we shall restrict ourselves to this component (see Section 4 for a discussion on this approximation). Therefore we have exactly two strings per inelastic collision. When the number of inelastic collisions experienced by a nucleon in a nuclear collision is larger than one, the extra strings (two per each extra collision) have sea quark constituents at the end corresponding to the multiply wounded nucleon. As explained in the Introduction, since strange sea quarks are present in the nucleon sea, the ratio of strange over non-strange particles will increase. One can object, however, that if the fraction S of strange quarks (defined in the Introduction) is the same as in the string breaking process, then the strings with sea quarks at their ends will produce the same strange over non-strange ratio as in the string breaking process - with no net strangeness enhancement. While true at asymptotic energies, this is not the case at present ones. For instance, let us consider the K^-/π^- ratio. In NN collisions at 200 GeV/c, the experimental value of this ratio is about 0.05. Since the values of S we consider are much larger, it is clear that the ratio K^-/π^- will increase. Another example is the ratio $\bar{\Lambda}/\bar{p}$ which,

as discussed in the Introduction, reaches a value close to 0.4 at Fermilab [7]. In the following we shall use the value $S = 0.5$. However, taking $S = 0.4$ changes very little our results [11].

The general formulae for the single particle inclusive rapidity distribution in nucleus-nucleus collisions is the following [9] :

$$\frac{dN^{AB}}{dy} = \frac{1}{\sigma_{AB}} \sum_{n_A,n_B,n} \sigma_{n_A,n_B,n} \Big\{ \theta(n_B - n_A) \Big[n_A \left(N^{qq_v^A - q_v^B}_{\mu_A,\mu_B}(y) + N^{q_v^A - qq_v^B}_{\mu_A,\mu_B}(y) \right) + (n_B - n_A) \left(N^{\bar{q}_s^A - q_v^B}_{\mu_A,\mu_B}(y) + N^{q_s^A - qq_v^B}_{\mu_A,\mu_B} \right) + (n - n_B) \left(N^{q_s^A - \bar{q}_s^B}_{\mu_A,\mu_B}(y) + N^{\bar{q}_s^A - q_s^B}_{\mu_A,\mu_B}(y) \right) \Big] + sym\ (n_A \leftrightarrow n_B) \Big\} \quad . \tag{2.1}$$

Here $\sigma^{AB}_{n_A,n_b,n}$ is the cross-section for n inelastic nucleon-nucleon collisions involving n_A and n_B participating nucleons, $\sigma_{AB} = \sum_{n_A,n_B,n} \sigma_{n,n_A,n_B}$ is the inelastic nucleus-nucleus cross-section, and $\mu_A = n/n_A$, $\mu_B = n/n_B$. $N(y)$ are the inclusive spectra of each individual string. Note that the total number of strings in Eq. (2.1) is $2n$ (two for each nucleon-nucleon collision).

In the following we restrict the discussion to the case $A = B$. Eq. (2.1) can be written in a simple, albeit approximate, form

$$\frac{dN^{A_P A_T}}{dy} = \bar{n}_A \left(N^{qq_v^P - q_v^T}_{\bar{\mu}_A,\bar{\mu}_A}(y) + N^{q_v^P - qq_v^T}_{\bar{\mu}_A,\bar{\mu}_A}(y) \right) + (\bar{n} - \bar{n}_A) \left(N^{q_s^P - \bar{q}_s^T}_{\bar{\mu}_A,\bar{\mu}_A}(y) + N^{\bar{q}_s^P - q_s^T}_{\bar{\mu}_A,\bar{\mu}_A}(y) \right) \quad . \tag{2.2}$$

Eq. (2.2) is obtained by neglecting the dependence of the string densities N on the μ's (which are replaced by their average values $\bar{\mu}$). The summations in (2.2) are then trivial - the numbers n_A and n being replaced by their average values $\bar{n}_A$ and $\bar{n}$. The approximate Eq. (2.2) is quite good at mid-rapidities. At large y

it becomes worse. However, in the rapidity region where the baryon densities are sizeable ($y^* \leq 2.5$), the errors involved are 5 to 10 %.

In Eqs. (2.1) and (2.2) only q_s-$\bar{q}_s$ pairs in the nucleon sea are considered. As discussed in the Introduction, we now assume that qq_s-$\bar{q}\bar{q}_s$ pairs are also present with relative fraction α. The modification in Eqs. (2.1) and (2.2) are straightforward. Eq. (2.2) is changed into :

$$\frac{dN^{A_P A_T}}{dy} = \bar{n}_A \left(N^{qq_v^P - q_v^T}_{\bar{\mu}_A,\bar{\mu}_A}(y) + N^{q_v^P - qq_v^T}_{\bar{\mu}_A,\bar{\mu}_A}(y) \right) + (\bar{n} - \bar{n}_A) \Big[(1-2\alpha) \left(N^{q_s^P - \bar{q}_s^T}_{\bar{\mu}_A,\bar{\mu}_A}(y) + N^{\bar{q}_s^P - q_s^T}_{\bar{\mu}_A,\bar{\mu}_A}(y) \right) + \alpha \left(N^{qq_s^P - q_s^T}_{\bar{\mu}_A,\bar{\mu}_A}(y) + N^{\overline{qq}_s^P - \bar{q}_s^T}_{\bar{\mu}_A,\bar{\mu}_A}(y) + N^{q_s^P - qq_s^T}_{\bar{\mu}_A,\bar{\mu}_A}(y) + N^{\bar{q}_s^P - \overline{qq}_s^T}_{\bar{\mu}_A,\bar{\mu}_A}(y) \right) \Big] \ . \tag{2.3}$$

In the following, we compute the rapidity distributions of Λ and $\bar{\Lambda}$ in nucleus-nucleus collisions using Eq. (2.3). The rapidity distributions of the individual strings are obtained by convoluting momentum distribution functions and fragmentation functions. All relevant formulae (including absolute normalization) are given in Appendix 1.

In numerical calculations we use the value $\alpha = 0.1$ taken from JETSET [18]. (A somewhat smaller value, $\alpha = 0.07$, is obtained in FRITIOF [16] and in BAMJET [19]). The values of $\bar{n}_A$ and $\bar{n}$ are obtained in the optical approximation of the Glauber model, with Saxon-Woods profiles, for impact parameter $|b| \leq 1$ fm. We get in SS collisions : $\bar{n}_A = 31$, $\bar{n} = 55$ and in Pb-Pb collisions $\bar{n}_A = 192$, $\bar{n} = 676$.

Before giving the numerical results, let us make some remarks concerning Eq. (2.3). Its first two terms are the same as in NN collisions - except for the value of $\bar{\mu}_A$ - which is 1 for NN, 2 for central SS and 4.5 for central Pb-Pb. The

third and fourth terms give negligeably small contributions to baryon-antibaryon production due to the large, $(m_\Lambda + m_{\bar{\Lambda}})^2$, thresholds in the short q_s-$\bar{q}_s$ strings. The remaining terms contain the contribution of sea diquarks and produce Λ and $\bar{\Lambda}$ by pairs. Detailed formulae for the rapidity distributions of baryons and antibaryons resulting from the various terms of Eq. (2.3) are given in Appendix 1.

In Fig. 1 we give the Feynman x distributions of Λ and $\bar{\Lambda}$ in pp collisions. They are obtained from the first two terms of Eq. (2.3) (i.e. from the sum of the contributions of the two qq-q valence-valence strings) with $\bar{\mu}_A = 1$. As shown previously in Ref. [20], the agreement with available data is quite good. Note that the shape of the fragmentation functions is determined from Regge intercepts (see Ref. [20] and Appendix 1).

The corresponding rapidity distributions in central SS collisions are given in Figs. 2 and 3. We see that the yields of both Λ and $\bar{\Lambda}$ are smaller than the data. The Λ yield, in particular, is considerably smaller than the experimental one. Therefore, we need a mechanism to produce extra Λ's. As already mentioned in the Introduction this can be achieved by a final state interaction of co-moving secondaries $\pi + N \to K + \Lambda$ ($K^* + \Lambda$, ...). A smaller number of $\bar{\Lambda}$ will also be produced via $\pi + \bar{N} \to K + \bar{\Lambda}$ ($K^* + \bar{\Lambda}$, ...). In the next section we discuss in detail these final state interactions.

3. The Final State Interaction of Secondaries

In independent string models, it is assumed that secondaries produced in different strings are independent from each other. Introducing a final state interaction of secondaries represents a departure from the independent string picture. In fact,

it corresponds to the simplest form of string interaction. It should be stressed that it is not known how to treat quantitatively such an interaction. Here we adopt the formalism introduced in Ref. [21]. Note that, at moderate energies, such a treatment of string interaction can be justified in the framework of Reggeon Field Theory [22].

Let us consider the number of Λ's produced by unit of space time volume d^4x resulting from the interaction $\pi + N \to K + \Lambda$ ($K^* + \Lambda$, ...). One has [21]

$$\frac{dN^\Lambda}{d^4x} =< \sigma > \rho_\pi(x)\ \rho_p(x) \tag{3.1}$$

where $\rho(x)$ are space-time dependent particle densities and $< \sigma >$ is the interaction cross-section - properly averaged over the momentum distributions of the colliding particles. We take $< \sigma >= 1.5$ mb which is the value of $\pi^- + p \to K^0 + \Lambda/\Sigma^0$ at its maximum near threshold. Beyond the threshold these two-body cross-sections decrease rapidly but quasi two-body interactions convert this sharp decrease into a mild increase.

We use cylindrical space-time variables : the longitudinal proper time is $\tau = \sqrt{t^2 - z^2}$ and the space-time rapidity $y = \frac{1}{2}\ell n \left[\frac{t+z}{t-z}\right]$. In these variables $d^4x = \tau\ d\tau\ dy\ d^2s$, where $\vec{s}$ is the transverse coordinate and d^2s an element of transverse area. As customary, we assume boost invariance - i.e. that the space-densities $\rho_i(x)$ are independent of y - and assume, furthermore, that the dilution in time of the density is mainly due to longitudinal motion. With this two assumptions we have [21] :

$$\rho_i(\tau, y, \vec{s}) = \rho_i(\tau, \vec{s})\frac{\tau_0}{\tau} \quad . \tag{3.2}$$

Using (3.2) it is trivial to integrate Eq. (3.1) on the variable τ. One gets

$$\frac{dN_\Lambda}{dy} = \int d^2s \frac{dN_\pi}{dy\ d^2s} \frac{dN_p}{dy\ d^2s}\ 3 < \sigma > \ell n\left[(\tau + \tau_0)/\tau_0\right] \tag{3.3}$$

where τ_0 is the formation proper time and τ the time during which the final interaction takes place. We take $\tau_0 = 1$ fm and $\tau = 3$ fm - based on interferometry measurements which indicate a very short time of particle emission and a freeze out time $\tau_0 + \tau \sim 4$ fm [23]. The factor 3 results from the product of three pion times two nucleon species, divided by a factor 2 - which is due to the fact that one out of two πN combinations have a negligeably small cross-section. For instance among the $\pi^\pm p$ combinations only $\pi^- p$ has to be considered.

Let us now explain how to compute $dN_i/dy\ d^2s$ in Eq. (3.3). The formulae given in Section 2 (see for instance Eq. (2.3)) give the expression of dN/dy - which is the result of integrating $dN/dy\ d^2s$ over d^2s. Actually, the only dependence on $\vec{s}$ is in the average values $\bar{n}_A$, $\bar{n}_B$ and $\bar{n}$. In the Glauber model, these average quantities are known as a function of $\vec{b}$ and $\vec{s}$. In the optical approximation one has

$$\bar{n}(\vec{b},\vec{s}) = \frac{AB\sigma}{\sigma_{AB}} T_A(\vec{b}-\vec{s})\ T_B(\vec{s}) \quad , \tag{3.4}$$

and

$$\bar{n}_A(\vec{b},\vec{s}) = \frac{A}{\sigma_{AB}} T_A(\vec{b}-\vec{s})\ \sigma_{NA}(\vec{s}) \tag{3.5}$$

where

$$\sigma_{NA}(\vec{s}) = 1 - (1 - \sigma\ T_A(\vec{s}))^A \quad .$$

Here σ is the nucleon-nucleon inelastic cross-section and $T_A(\vec{b})$ the nuclear profile - for which we use the standard Saxon-Woods expression. Clearly, when computing

the r.h.s. of Eq. (3.3) one has to perform the products $\bar{n}^2(\vec{b},\vec{s})$, $\bar{n}_A^2(\vec{b},\vec{s})$, $\bar{n}_A(b,\vec{s})$ $\bar{n}(b,\vec{s})$ and integrate them over both d^2s and d^2b. It is easy to see that such integrals of products are smaller than the product of integrals dN_π/dy times dN_p/dy and that the ratio of the former over the latter is roughly proportional to $R_A^{-2} \sim A^{-2/3}$. Therefore, the number of Λ's resulting from the final state interaction, will increase quite fast with increasing A. Indeed, at mid-rapidities, the product dN_π/dy times dN_p/dy increases with A approximately as $A^{8/3}$ and thus the number of Λ's increases approximately as A^2.

In order to compute the rapidity distributions of Λ resulting from the final state interaction (3.1) one has to compute first the densities of pions and protons. This has been done using the formulae in Appendix 1.

The rapidity distributions of h^- in NN, SS and Pb-Pb collisions are given in Figs. 4 and 5. The agreement with experiment is reasonable. Note that, due to the two string approximation in NN, the rapidity distribution tends to be too broad. Indeed, the contribution of the q_s-$\bar{q}_s$ strings, although small at 200 GeV/c, is concentrated at mid-rapidities. This is partly compensated by choosing steeper diquark fragmentation functions (see Appendix 1). In any case, our aim here is not to get the best possible description of h^- distributions, but only to have a reasonable form of dN_{π^-}/dy in order to use it in Eq. (3.1). Following Ref. 4, we have taken $dN_{\pi^-}/dy = 0.93\ dN_{h^-}/dy$.

The Feynman x distributions of proton and antiprotons in pp collisions are given in Fig. 6. The agreement with data is quite good. Note that diffractive dissociation, which produces a peak near $x = 1$ in the p distribution has not been included in the model. The corresponding results for peripheral and central SS collisions are

given in Fig. 7. Actually, both the data and the theoretical curves correspond to the difference $p-\bar{p}$. The shape of the rapidity distribution is well reproduced in the model for peripheral collisions but not for central ones. In the latter case, the shape of the experimental distribution is much flatter than the theoretical one. Note, however, that the average multiplicity is the same for the two distributions. This disagreement between an independent string model prediction and experiment is very significant and we are going to discuss it in some detail. First of all, in DPM the stopping power is entirely controlled by the momentum distribution functions. More precisely, when the average number of collisions per nucleon increases (i.e. when $\bar{\mu}_A$ in Eq. (2.3) increases), the maximum of the proton spectrum is shifted to smaller rapidities (see Fig. 2 of Ref. [24]). This effect is seen in Fig. 7. However, in central SS collisions $\bar{\mu}_A \sim 2$ and, therefore, the effect is small. Moreover, the decrease of the proton spectrum between its maximum and $y^* \sim 0$ is very steep even for a large number of inelastic collisions. Thus, the dramatic flattening of the proton rapidity distribution between peripheral and central SS collisions in Fig. 7 cannot be reproduced in the model, and, as discussed in the Introduction, rescattering of the produced nucleons is needed.

We can now compute the rapidity distribution of $\bar{\Lambda}$ resulting from the final state interaction $\pi + \bar{N} \to K + \bar{\Lambda}$ ($K^* + \bar{\Lambda}$, ...). The results are shown in Fig. 2. The agreement with experiment is quite good.

The corresponding results for Λ production, including the effect of the final state interaction $\pi + N \to K + \Lambda$ ($K^* + \Lambda$, ...), are given in Fig. 3 (dashed line). We see that the final state interaction has produced a substantial increase of the Λ yield, which is now in qualitative agreement with experiment. We conclude that

the main features of Λ and $\bar{\Lambda}$ production in central SS collisions can be understood in the scenario presented in this paper.

We turn next to central *Pb-Pb* collisions at 160 GeV/c per nucleon. In this case the rate of strange baryon production from the final state interactions is very high at mid-rapidities due to the large value of the pion density and one can not ignore any longer the crossed reactions $\pi + \Lambda \to K + N$ and $\pi + \bar{\Lambda} \to K + \bar{N}$. Indeed, it turns out that, at mid-rapidities, equilibrium between strange and non strange baryons is reached before the freeze out time $\tau_0 + \tau$ (assumed to be the same as in central SS collisions). When this equilibrium is reached one has $< n >_p + < n >_n = 1.6 < n >_\Lambda$ (where $0.6 < n >_\Lambda$ takes into account the $\Sigma^\pm$ baryons) and the strange baryon multiplicity does not increase any longer. The predictions for the rapidity distribution of $\bar{\Lambda}$ and Λ in central *Pb-Pb* are shown in Figs. 2 and 3 (upper lines scaled down by a factor 5).

A close look at Fig. 3 shows that the computed Λ distribution in SS collisions has a shallow dip at $y^* = 0$ which is not seen in the data. Probably this is related to the lack of baryon stopping discussed above and requires further rescattering of the produced Λ's. In order to have a rough estimate of the effect of the baryon rescattering, we have introduced some extra stopping in the proton spectrum (without changing the proton average multiplicity) by shifting it by $\Delta y = 0.5$. The modified $p - \bar{p}$ rapidity distribution is shown in Fig. 7 (full upper line). Using such shifted proton distributions in Eq. (3.3), we obtain a flatter Λ distribution both in SS and *Pb-Pb* collisions (full lines in Fig. 3), which for SS collisions is in good agreement with experiment.

Finally, the average multiplicities of pions, kaons, protons lambdas and anti

lambdas in SS and Pb-Pb collisions are given in Table 1. (A discussion of cascades and omega production in the present framework can be found in Refs. 10, 11). We observe that the ratio $\bar{\Lambda}/h^-$ (Λ/h^-) increase by about 50 % (70 %) between SS and Pb-Pb collisions.

4. Conclusions

We have studied meson and baryon strangeness enhancement in an independent string model with quark-antiquark and diquark-antidiquark pairs in the nucleon sea. The expe rimental data have forced us to depart from string independence and to introduce a final state interaction of co-moving secondaries. The necessity of final state rescattering also follows from the study of the shape of the proton rapidity distribution in central SS collisions. Final state interactions are the simplest forms of string interaction - which is a first step in order to drive the system toward equilibrium. Using all these ingredients, we have obtained a reasonable agreement with experiment. We feel that a more accurate description is not possible in the present state of the art.

The present model has many uncertainties that we want to discuss briefly. Apart from the poor knowledge of the parameter S and α, there is an uncertainty resulting from the hadronization of short strings and, in particular, of strings involving sea diquarks (see Appendix 1). Furthermore, the introduction of final state interactions rises a lot of questions. Not only a rigourous treatment of the final state interaction does not exist, but, moreover, we can not be sure that other reactions (for most of which the cross-sections are not even known) do not affect our results. (In particular we have neglected annihilation reactions of nucleons and antilambdas or antinucleons and lambdas which have a very large cross-section at

threshold. However, this cross-section drops very fast after the threshold and the corresponding value of $< \sigma >$ in Eqs. (3.1), (3.3) is not known). Despite all these drawbacks, the effects discussed in the present work are important and cannot be ignored in strangeness enhancement studies.

A characteristic feature of the model presented here is that it predicts a continuous strangeness enhancement, not only from proton-proton to proton-nucleus and to average (i.e. minimum-bias) nucleus-nucleus collisions, but also in proton-proton when energy or event multiplicity is increased. Of course to get this latter effect it is necessary to give up the two string approximation in pp collisions. This assumption is of no consequence for the results presented here, provided a good description of pp data is achieved [25]. Indeed the results for nucleus-nucleus collisions are determined by the input in pp (or rather NN) collisions. However, when multistrings are introduced, one obtains [26] an increase of the ratio K/π in pp collision when increasing either the energy or the event multiplicity, as observed experimentally. Moreover, the increase with energy [7] of the ratio $\bar{\Lambda}/\bar{p}$, can also be understood in this way. Note, however, that the contribution to strangeness enhancement resulting from the final state interaction (which is very important for Λ production) is most effective in central nucleus-nucleus collisions where the densities of secondaries are very large.

In conclusion, the study of strangeness enhancement is a very active field. This is clear from the large number of recent work on the subject [1]. Actually, during the latest stages of the present work [27] many interesting papers on this subject have appeared in the literature [28-31]. Some of them give also predictions for Pb-Pb collisions. The theoretical ideas in these papers and their predictions are, in

general, quite different from ours. Forthcoming results with a lead beam at CERN will certainly trigger more activity and give new insight into this very interesting field. Predictions for RHIC and LHC energies are also needed.

Acknowledgements :

We would like to thank A. Krzywicki for useful discussions. We also thank J. Ranft for an ongoing collaboration on this subject.

One of the authors (C. M.) has benefitted of a EEC postdoctoral project ER-BCHBI CT 930 547.

This work has been done with the help of an INTAS contract 93-0079.

Appendix 1

Hadron Spectra of Individual String

Both in DPM and QGSM the hadron spectra of the individual strings are given by a convolution of structure functions and fragmentation functions. In DPM, one has for the rapidity density $N^{qq-q}(y,s)$ of hadron h in, say, a diquark-quark string :

$$N^{qq-q}_{\mu_1,\mu_2}(y,s) = \int_0^1 dx_1 \int_0^1 dx_2 \; \rho^{qq}_{\mu_1}(x_1) \; \rho^{q}_{\mu_2}(x_2)$$

$$\frac{dN^{qq-q}}{dy}(y-\Delta, s_{str.}) \; \theta(s_{str.} - s_{thr.}) \quad . \qquad (A.1)$$

Here $\rho^{qq}_{\mu_1}$ and $\rho^{q}_{\mu_2}$ are the momentum distribution functions of diquark and quark which depend on the light cone momentum fractions x_1 and x_2. The index μ_1 (μ_2) denotes the number of inelastic collisions suffered by the nucleon to which the diquark (quark) belongs. The squared invariant mass of the string is $s_{str} = x_1 x_2 s$ and $\Delta = 1/2 \log[x_1/x_2]$ is the rapidity distance between the C. of M. of the string and the overall C. of M. At fixed values of x_1 and x_2 the string hadronization is just given in terms of qq and q fragmentation functions :

$$\frac{dN^{qq-q}}{dy}(y-\Delta, s_{str.}) = \begin{cases} G^h_{qq}(y) & \text{for } y \geq \Delta \\ G^h_q(y) & \text{for } y \leq \Delta \end{cases} \qquad (A.2)$$

where $G(y)$ are fragmentation functions (see below). Of course $dN^{qq_v-q_v}/dy = 0$ for y outside the rapidity interval determined by the string endpoints. Note the presence of a threshold θ-function in Eq. (A.2). The value of s_{thr} corresponds to the squared mass of the lightest system that can be produced in association with the triggered hadron h*.

* For instance for a qq_v-q_v string fragmenting into a Λ we have $s_{thr} = (m_\Lambda +$

An important feature of DPM and QGSM is the fact that the structure function is determined in terms of Regge intercepts. In DPM, the structure function in the presence of $2k$ such constituents is given by [9] :

$$\rho_k(x_1 \cdots x_{2k}) = C_{2k}\ x_1^{-1/2} x_2^{-1} \cdots x_{2k-1}^{-1} x_{2k}^{3/2} \delta\left(1 - \sum_{i=1}^{2k} x_i\right) \quad . \qquad (A.3)$$

The index 1 refers to the valence quark and the index $2k$ to the diquark. All other indices refer to sea quarks and antiquarks. The constant C_{2k} is obtained from the normalization of ρ_{2k} to unity. The structure function of each individual constituent, which appears in Eq. (A.1), is obtained by integrating (A.3) over the variables of all other constituents. (In actual calculations the singular factor x^{-1} is replaced by $\bar{x}^{-1}$ with $\bar{x} = (x^2 + \mu^2/s)^{1/2}$, and $\mu = 0.1$ GeV ; varying μ between 0.05 and 0.3 produces only minor changes in our results).

In QGSM the formulae are somewhat different [7]. The diquark and quark fragment independently from each other and the threshold resulting from the θ-function in (A.1) is not present. Moreover in Eq. (A.3) sea quarks are assumed to have, at present energies, a $x^{-1/2}$ behaviour at $x \sim 0$ - the same as for valence quarks. In this case the integration of ρ in (A.3) over all variables except one can be performed analytically. One gets

$$\rho_{2k}^{q}(x) = C_{2k}^{q}\ x^{-0.5}(1-x)^{2k+1/2}$$
$$\rho_{2k}^{qq}(x) = C_{2k}^{qq}\ x^{1.5}(1-x)^{2k-3/2} \quad . \qquad (A.3')$$

$m_K)^2$. For that of a us-d string we have $s_{thr} = m_\Lambda^2$. Likewise for pion (kaon) production in a $u\bar{d}$ ($s\bar{d}$) string we have $s_{thr} = \mu_\pi^2 (m_K^2)$ - where μ_π is the pion transverse mass.

The coefficients C are determined (analytically) from the normalization to unity of $\rho(x)$. Note that the $\bar{x}^{-1}$ behaviour in DPM strongly reduces the probability of a sea quark to cross to the opposite hemisphere (as compared to an x^{-1} behaviour, which corresponds to a flat distribution in rapidity). As a consequence, the results obtained in DPM and QGSM are quite similar - at least at the energies considered here.

In the first DPM papers, fragmentation functions were just derived from a fit to pp (or e^+e^-) data. An important break through was achieved when it was realized that, not only momentum distribution functions, but also fragmentation functions could be derived in terms of Regge intercepts [7]. In this way the predictivity of the model was greatly increased. Indeed, it has been possible to predict the shape of the rapidity distributions of π, K, p, Λ, etc in pp collisions - with absolute rates as the only free parameters.

In the following, we use the fragmentation functions of baryons and antibaryons obtained in this way. More precisely, the form of the fragmentation functions for Λ and $\bar{\Lambda}$ are given by [20]

$$
\begin{aligned}
D_u^{\bar{\Lambda}} &= D_d^{\bar{\Lambda}} = \frac{1}{Z}(1-Z)^{3.5} \\
D_u^{\Lambda} &= D_d^{\Lambda} = \frac{1}{Z}(1-Z)^{2.5} \\
D_{uu,2}^{\bar{\Lambda}} &= D_{ud,2}^{\bar{\Lambda}} = D_{dd}^{\bar{\Lambda}} = \frac{1}{Z}(1-Z)^{5.5} \\
D_{uu,2}^{\Lambda} &= D_{dd,2}^{\Lambda} = D_{ud,2}^{\Lambda} = (1-Z)^{6.5} \quad .
\end{aligned}
\tag{A.4}
$$

Here $D_{qq,2}$ denotes the fragmentation of a diquark into a non-leading baryon. We have to add to it a (dominant) term, $D_{qq,1}$, corresponding to leading baryon pro-

duction, given by

$$D^{\Lambda}_{uu,1} = D^{\Lambda}_{dd,1} = \frac{1}{Z} Z^{1.5}(1-Z)^{1.5} \quad ; \quad D^{\Lambda}_{ud,1} = \frac{1}{Z} Z^{1.5}(1-Z)^{0.5} \quad . \qquad (A.5)$$

Turning to p and $\bar{p}$ production, we have [20]

$$\begin{aligned} D^{\bar{p}}_{u} &= D^{\bar{p}}_{d} = \frac{1}{Z}(1-Z)^3 \\ D^{p}_{u} &= \frac{1}{Z}(1-Z)^2 \quad ; \quad D^{p}_{d} = \frac{1}{Z}(1-Z)^2 \left[\frac{1}{3} + \frac{2}{3}(1-Z)\right] \\ D^{\bar{p}}_{dd,2} &= D^{\bar{p}}_{uu,2} = D^{\bar{p}}_{ud,2} = \frac{1}{Z}(1-Z)^5 \\ D^{p}_{dd,2} &= D^{p}_{uu,2} = D^{p}_{ud,2} = \frac{1}{Z}(1-Z)^6 \end{aligned} \qquad (A.6)$$

and, for the leading proton,

$$D^{p}_{ud,1} = \frac{1}{Z} Z^{1.5}(1-Z)^0 \quad ; \quad D^{p}_{uu,1} = \frac{1}{Z}(1-Z)^0 \quad . \qquad (A.7)$$

Finally for neutron production we have

$$\begin{aligned} & D^{n}_{u} = D^{p}_{d} \quad ; \quad D^{n}_{d} = D^{p}_{u} \quad , \quad D^{n}_{uu,2} = D^{p}_{uu,2} \quad , \\ & D^{n}_{ud,1(2)} = D^{p}_{ud,1(2)} \quad , D^{n}_{uu,1} = \frac{2}{3Z} Z^{1.5}(1-Z)^1 \quad . \end{aligned} \qquad (A.8)$$

The values of all powers of Z and $1-Z$ in Eqs. (A.4)-(A.8) are determined in terms of Regge intercepts*. For example, the power 0 of $1-Z$ in Eq. (A.7) is given by $-\alpha_R(0) + \lambda$ where $\alpha_R(0) = 0.5$ is the dominant reggeon intercept and

* The only factors which are not determined in this way are the factor $[1/3 + 2/3(1-Z)]$ in Eq. (A.6) and the factor $2/3$ in Eq. (A.8). These factors have a trivial origin. For instance the factor in (A.6) results from the fact that the fragmentation of u and d quarks into a proton is the same at $Z \to 0$. However, at $Z \to 1$ the

$\lambda = 2\alpha' p_\perp^2 \simeq 0.5$ is common to all fragmentation functions and results from the integration over transverse momentum. In the case of Λ production $D^\Lambda_{ud,1}$ has a softer $Z \to 1$ behaviour, with a power $-\alpha_\phi(0)+\lambda = 0.5$, which explains the different shape of Λ and p (non-diffractive) rapidity distributions (see Figs. 1 and 6). Of course, there are some numerical uncertainties in the determination of these powers - in particular in the power of Z in the leading baryon fragmentation function. The value 1.5 used above has been chosen, within the theoretically allowed range, in order to obtain the best description of the pp data in the DPM formalism.

The only remaining point is to define the functions G_{qq} and G_q in the r.h.s. of Eq. (A.2), in terms of the fragmentation functions defined above. This is done in the following way. Let us consider first the production of antibaryons and non-leading baryons. In this case we have

$$G^h_{qq,2}(y) = \bar{a}_h \; Z_+ \; D^h_{qq,2}(Z_+) \; Z_- \; D^h_q(Z_-) \quad , \qquad \text{for } y \geq \Delta$$
$$G^h_{q,2}(y) = \bar{a}_h \; Z_- \; D^h_q(Z_-) \; Z_+ \; D^h_{qq,2}(Z_+) \quad , \qquad \text{for } y \leq \Delta \quad . \qquad (A.9)$$

Here Z_+ and Z_- are the light cone momentum fractions defined as $Z_+ = \exp(y^{str} - y^{str}_{MAX})$, $Z_- = \exp(-y^{str} - y^{str}_{MAX})$, where $y^{str} = y - \Delta$ and y^{str}_{MAX} is the maximal rapidity that a hadron h can have in the string (for fixed values of the momentum fractions x_1 and x_2 of the string ends). Note that for a string with a very large in-

---

fragmentation of a u-quark is three times larger since the three combinations $u(ud)$, $u(du)$ and $u(uu)$ are possible. (The later will give a Δ^{++} which will often decay into a proton). On the contrary, for the fragmentation of a d quark the only possible combination is $d(uu)$. Likewise, the fragmentation of a diquark uu into a leading neutron is only possible through diquark breaking and has a probability of 2/3 as compared to the corresponding one for a ud diquark.

variant mass $Z_- \sim 0$ for $y \geq \Delta$ and therefore $G^h_{qq,2}(y) \sim \bar{a}_h \; Z_+ \; D^h_{qq}(Z_+)$. Likewise, for $y \leq \Delta$, $Z_+ \sim 0$ and $G^h_{q,2}(y) \sim \bar{a}_h \; Z_- \; D^h_q(Z_-)$.

In the case of a leading baryon, Eq. (A.2) has to be modified. We have

$$\frac{dN^{qq-q}}{dy}\,(y-\Delta, s_{str}) = G_{qq,1}(y) \qquad (A.2')$$

for both $y \geq \Delta$ and $y < \Delta$, with

$$G^h_{qq,1}(y) = a_h \; Z_+ \; D^h_{qq,1}(Z_+) \quad , \qquad (A.10)$$

when the diquark is located in the positive rapidity hemisphere. In the opposite case one has to replace Z_+ by Z_-. Note that, when the string invariant mass is large, one has $Z_+ \; D^h_{qq,1}(Z_+) \sim 0$ in the backward hemisphere and, therefore, the leading baryon distribution is concentrated on the diquark side - as it should be. A further modification is necessary in order to preserve baryon number conservation. Eqs. (A.1) (A.2') do not satisfy this property - a main source of violation being the threshold factor. Actually, a non Monte Carlo formalism which leads to exact baryon conservation has not been found so far. However, a good numerical accuracy in this conservation law is achieved by dividing the r.h.s. of Eq. (A.1) by

$$D = \int_0^1 dx_1 \int_0^1 dx_2 \; \rho(x_1) \; \rho(x_2) \; \theta\,(s_{str} - s_{thr}) \quad . \qquad (A.11)$$

This device to enforce baryon number conservation must be used only for leading baryon production.

The normalization factors a_h and $\bar{a}_h$ have been determined in order to reproduce the measured rapidity distributions of baryons and antibaryons. We have :

$$a_p = 0.82 \quad , \quad \bar{a}_p = 0.036 \quad , \quad a_\Lambda = 0.17 \quad , \quad a_{\bar{\Lambda}} = 0.012 \quad . \qquad (A.12)$$

Note that the same normalization constant $\bar{a}$ is used for antibaryons and for non-leading baryons.

Plugging the above expressions for the rapidity distributions of the individual strings in Eq. (2.3) we can compute the baryon and antibaryon rapidity distributions in nucleus-nucleus collisions. The only missing ingredients are the fragmentation functions of the strange sea diquarks us, ds and ss. For these functions we use the following approximate relations

$$D^{\Lambda}_{us,1} = D^{\Lambda}_{ds,1} = D^{\bar{\Lambda}}_{\bar{u}\bar{s},1} = D^{\bar{\Lambda}}_{\bar{d}\bar{s},1} = D^{p}_{ud,1} \quad ,$$

$$D^{\Lambda}_{ss,1} = D^{\bar{\Lambda}}_{\bar{s}\bar{s},1} = D^{n}_{uu,1} \quad . \qquad (A.13)$$

Although everything is now fully especified in order to compute baryon and antibaryon rapidity distributions, we give, as an illustration, the detailed form of the fragmentation of a qq_s-q_s string into a leading Λ (which is, of course, identical to that of an $\bar{\Lambda}$ in a $\bar{q}\bar{q}_s$-$\bar{q}_s$ string). We have

$$N^{qq_s^P - q_s^T}_{\bar{\mu}_A, \bar{\mu}_A}(y) = \frac{1}{D}\int_0^1 dx_1 \int_0^1 dx_2 \; \rho^{q_s}_{\bar{\mu}_A}(x_1) \; \rho^{q_s}_{\bar{\mu}_A}(x_2) \; G^{\Lambda}_{qq,1}(y) \; \theta\left(s_{str} - s_{thr.}\right) \quad (A.14)$$

where

$$G^{\Lambda}_{qq,1}(y) = \frac{4}{(2+S)^2} a_{\Lambda} Z_+ \left(\frac{2}{3} D^{\Lambda}_{ud,1}(Z_+) + \frac{1}{3} D^{\Lambda}_{uu,1}(Z_+) \right) +$$

$$\frac{4S}{(2+S)^2} a_p \; Z_+ \; D^{p}_{ud,1}(Z_+) + \frac{S^2}{(4+S)^2} a_p \; Z_+ \; D^{n}_{uu,1}(Z_+) \quad . \qquad (A.15)$$

Eq. (2.4) is obtained from (A.1) after dividing by the denominator in (A.11). Note that the ρ function of the sea diquark is taken to be the same as the corresponding one of a sea quark. In Eq. (2.5) we have explicitly written the contributions of the non-strange sea diquarks (terms proportional to a_{Λ}) and that of the strange

sea diquarks (terms proportional to a_p). The contribution of the non-strange sea diquarks (uu, dd, ud and du) is proportional to $4/(2+S)^2$. That of the diquarks containing one strange quark (us, ds, su and sd) is proportional to $4S/(2+S)^2$, and that of the diquark ss to $S^2/(2+S)^2$. For the fragmentation functions of the strange sea diquarks we have used Eqs. (A.13).

Note that for the baryon production in strings containing sea diquarks we have used the same prescription as for valence diquarks, namely we have divided by the denominator D (see Eqs. (A.11) and (A.14)) - although, in this case, this is not required by baryon number conservation since baryons are produced by pairs. Without dividing by D the production of Λ and $\bar{\Lambda}$ from sea diquark strings would have been substantially smaller. Actually, we regard the hadronization of the sea diquark strings as the main source of uncertainty in this approach.

Turning next to the production of p and $\bar{p}$, we have to replace in Eq. (A.14), $G^{\Lambda}_{qq,1}$ by

$$G^{p}_{qq,1}(y) = \frac{4}{(2+S)^2} a_p \left[\frac{2}{3} D^{p}_{ud,1}(Z_+) + \frac{1}{6} D^{p}_{uu,1}(Z_+) + \frac{1}{6} D^{p}_{dd,1}(Z_+) \right] \quad . \qquad (A.16)$$

In this case, the contribution coming from the fragmentation of strings containing strange sea diquarks turns out to be very small and has been neglected.

In order to compute the final state interaction of secondaries (pions and nucleons) introduced in Section 3, we also need the rapidity distribution of h^-. In this case the contribution of the q-$\bar{q}$ strings is not negligeable and has the effect of narrowing the rapidity distribution. For our present purpose, however, it is enough to consider the two valence strings, provided the fragmentation function of valence quark and diquark are chosen in such a way as to reproduce the $NN \to h^-$ distribution. As expected from the absence of q-$\bar{q}$ strings, the diquark fragmentation

functions have to be softer than expected from Regge arguments. (Of course this drawback disappears when multistrings are introduced [32]). We take

$$G_{ud}^{\pi^-}(y) = a_{h^-}(1-Z)^4 \quad ; \quad G_{uu}^{\pi^-} = a_{h^-}(1-Z)^5 \quad G_{dd}^{\pi^-} = a_{h^-}(1-Z)^4 \qquad (A.17)$$

where

$$Z = |2\mu_\pi \sinh(y-\Delta)/\sqrt{s_{str}}| \quad ,$$

and μ_π is the transverse pion mass. The normalization, chosen to reproduce the rapidity plateau height in NN collisions, is $a_{h^-} = 0.59$. For the quark fragmentation functions we take the ones introduced in Refs. [33], namely

$$\begin{aligned} G_d^{h^-}(y) &= \frac{a_{h^-}}{1.35}(1+Z)\ F(Z) \\ G_d^{h^+}(y) &= \frac{a_{h^-}}{1.35}(1-Z)\ F(Z) \end{aligned} \qquad (A.18)$$

where

$$F(Z) = \frac{1.3(1-Z)^2 + 0.05}{1-0.5Z} \quad .$$

Actually, in computing the h^- rapidity distribution in AA collisions, we have used Eq. (2.2), i.e. the expression without sea diquarks. More precisely, we take

$$\begin{aligned} \frac{dN_{h^-}^{A_P A_T}}{dy} &= \bar{n}_A \left(N_{\bar{\mu}_A,\bar{\mu}_A}^{qq_v^P - q_v^T}(y) + N_{\bar{\mu}_A,\bar{\mu}_A}^{q_v^P - qq_v^T}(y) \right) + \\ & (\bar{n} - \bar{n}_A)\frac{2}{2+S}\left(N_{\bar{\mu}_A,\bar{\mu}_A}^{q_s^P - \bar{q}_s^T}(y) + N_{\bar{\mu}_A,\bar{\mu}_A}^{\bar{q}_s^P - q_s^T}(y) \right) \end{aligned} \qquad (A.19)$$

In Eq. (A.19) we only consider the contribution of the non-strange sea strings. Of course some pions are also produced in strange sea ones. However their contribution is small and roughly compensates the loss of pions resulting from the introduction

of sea diquark strings (see Section 2), where pion production is smaller than in q_s-$\bar{q}_s$ strings.

Finally, to compute the kaon multiplicities (Table 1), we have used the experimental values in NN collisions [6] and have assumed 11] that the fragmentation $s \to K^+$ ($\bar{s} \to K^-$) is equal to $u \to \pi^+$ ($d \to \pi^-$). This is, of course, justified only at the first string break-up. However, due to the small momentum fraction carried by the sea quark the probability of further break-ups in the rapidity hemisphere of the sea quark is negligeably small.

References

[1] See Proceedings of S'95 Conference, Tucson, January 1995.

[2] B. Koch, B. Muller and J. Rafelski, Phys. Rep. **142** (1986) 167.

[3] R. Salmeron, Nucl. Phys. **A566** (1994) 199c.

[4] NA35 Collaboration : T. Alber et al., Z. Phys. **C64** (1994) 195.

[5] E755 Collaboration : N. N. Biswas, Proceedings XXI International Symposium on Multiparticle Dynamics, World Scientific (1992).

[6] M. Gazdzicki and Ole Hansen, Nucl. Phys. **A528** (1991) 754.

[7] E765 Collaboration : T. Alexopoulos et al., Phys. Rev. **D46** (1992) 2773.

[8] NA36 Collaboration : J. M. Nelson, Nucl. Phys. **A566** (1994) 217c.

[9] A. Capella, U. Sukhatme, C. I. Tan and J. Tran Thanh Van, Phys. Rep. **236** (1994) 225.

[10] J. Ranft, A. Capella, J. Tran Thanh Van, Phys. Lett. **B320** (1994) 346 ;

H. J. Möhring, J. Ranft, A. Capella, J. Tran Thanh Van, Phys. Rev. **D47** (1993) 4146 (the calculations in these papers are based on the DPMJET and DTNUC codes).

[11] A. Capella, Orsay preprint LPTHE 94-113.

[12] QGSM : A. Kaidalov, Phys. Lett. **B117** (1982) 459 ; A. Kaidalov and K. A. Ter-Martirosyan, Phys. Lett. **B117** (1982) 247. For the corresponding Monte Carlo code see N. S. Amelin et al., Phys. Rev. **C47** (1993) 2299 ; N. S. Amelin et al, Nucl. Phys. **A544** (1992) 463c.

[13] A.D. Martin, R. G. Roberts and W. J. Stirling, preprint RAL-94-005 (DTP/94/3).

[14] N. Armesto, M.A. Braun, E.G. Ferreiro and C. Pajares, University of Santiago de Compostela, preprint US-FT/16-94. References to earlier papers on string fusion can be found in G. Gustafson, Nucl. Phys. **A566** (1994) 233c.

[15] RQMD : H. Sorge, R. Matiello, A. von Kectz, H. Stöcker and W. Greiner, Z. Phys. **C47** (1990) 629 ; H. Sorge, M. Berenguer, H. Stöcker and W. Greiner, Phys. Lett. **B289** (1992) 6 ; Th. Schönfeld et al, Nucl. Phys. **A544** (1992) 439c.

[16] FRITIOF : B. Andersson, G. Gustafson and B. Nilsson-Almquist, Nucl . Phys. **B 281** (1987) 289 ; B. Nilsson-Almquist, E. Stenlund, Comp. Phys. Comm. **43** (1987) 387. In this code the enhancement of Λ and $\bar{\Lambda}$ is essentially due to the final state interaction (B. Andersson, private communication).

[17] NA35 Collaboration : H. Ströbele et al., Nucl. Phys. **A525** (1991) 59c.

[18] JETSET : T. Sjöstrand, CERN Report CERN-TH 6488/92, 1992.

[19] BAMJET : S. Ritter, Comput. Phys. Commun. **31** (1984) 393.

J. Ranft and S. Ritter, Acta Phys. Pol. **B11** (1980) 259.

[20] A. B. Kaidalov and O. I. Piskunova, Z. Phys. **C30** (1986) 141.

[21] P. Koch, U. Heinz and J. Pitsut, Phys. Lett. **B243** (1990) 149.

[22] K. G. Boreskov, A. B. Kaidalov, S. M. Kiselev and N. Ya Smorodinskaya, Sov. J. Nucl. Phys. **53** (1991) 356.

[23] NA35 Collaboration : G. Roland, Nucl. Phys. **A566** (1994) 527c ; D. Ferenc, Proceedings XXIX Rencontres de Moriond (1994) ed. J. Tran Thanh Van ;

NA44 collaboration : T.J. Humanic, Nucl. Phys. **A566** (1994) 115c ; S. Panday, Proceedings Rencontres de Moriond, ibid.

[24] A. Capella, J. A. Casado, C. Pajares, A. V. Ramallo and J. Tran Thanh Van, Z. Phys. **C33** (1987) 541.

[25] For Monte Carlo analysis of strangeness enhancement in the present approach, including multistrings in *pp* collisions, see J. Ranft, A. Capella and J. Tran Thnah Van, in preparation.

[26] J. Ranft, preprint LNF 94/035 P.

[27] A short description of the results of the present work was given in A. Capella et al., Proceedings XXX Rencontres de Moriond, Les Arcs (France), 1995, presented by C. Merino.

[28] T. S. Biró, P. Levai and J. Zimányi, preprint RIPNP, Budapest (1995) and Ref. 1.

[29] P. Lévai and Xin-Nian Wang, preprint RIPNP, Budapest and Ref. 1.

[30] C. Slotta, J. Sollfrank and U. Heinz preprint TPR-95-04.

[31] K. Kadija, N. Schmitz and P. Seyboth, MPI-PhE/95-07.

[32] A. B. Kaidalov and O. I. Piskunova, Sov. J. Nucl. Phys. **41** (1985) 816.

[33] A. Capella and J. Tran Thanh Van, Z. Phys. **C10** (1981) 249.

[34] NA35 Collaboration : D. Röhrich, Nucl. Phys. **A566** (1994) 35c.

[35] NA35 Collaboration : T. Alber et al., Proceedings XXX Rencontres de Moriond, Les Arcs, France (1995).

[36] A. E. Brenner et al., Phys. Rev. **D26** (1982) 1497.

Figure Captions

Fig. 1 Feynman x distributions of Λ and $\bar{\Lambda}$ produced in pp collisions at 200 GeV/c. The compilation of experimental data, at energies ranging from 100 GeV/c to $\sqrt{s} = 63$ GeV, is from Ref. 20. Error bars in the Λ data are only shown for $x = 0.2$ and 0.95.

Fig. 2 Rapidity distribution of $\bar{\Lambda}$ in central SS collisions at 200 GeV/c per nucleon (dashed line) compared to the data of Ref. 4. The dashed-dotted line is the corresponding result without final state interaction. The full line is the prediction for central Pb-Pb at 160 GeV/c per nucleon, scaled down by a factor 5.

Fig. 3 Rapidity distribution of Λ in central SS collisions at 200 GeV/c per nucleon (full and dashed lines) compared to the data of Ref. 4. The dashed-dotted line is the corresponding result without final state interaction. The dashed (full) line is obtained by adding the final state interaction, Eq. (3.3), with the proton spectrum corresponding to the dashed (full) lines in Fig. 7. The upper lines are the predictions for central Pb-Pb collisions at 160 GeV/c per nucleon scaled down by a factor 5. The dashed (full) line is computed by adding the final state interaction with the proton spectrum computed in DPM (shifted by $\Delta y = 0.5$).

Fig. 4 The rapidity distribution of negative hadrons (h^-) in central SS collisions (full line) and in N-N collisions (dashed line), the latter scaled up by a factor 32, compared to the data of Ref. [34].

Fig. 5 Rapidity distribution of negative hadrons (h^-) in central Pb-Pb collisions at 160 GeV/c per nucleon. The data are from Ref. [35].

Fig. 6 Feynman x distributions of proton and antiprotons in pp collisions at 200 GeV, compared with the data of Ref. [36] at 175 GeV/c. Diffraction is not included in the model calculation.

Fig. 7 Rapidity distribution of proton minus antiproton in peripheral (full line) and central (full and dashed lines) SS collisions compared with data from Ref. [17]. The theoretical curve for the peripheral case corresponds to $N + N \rightarrow (p - \bar{p}) + X$, normalized to the data. The dashed line in SS is the result of DPM. The full line in SS is obtained by adding some extra stopping to the proton (with $\Delta y = 0.5$) without changing the proton average multiplicity (see main text).

	NN	NN	SS	SS	SS	Pb-Pb	Pb-Pb
		experiment [6]	DPM	DPM + f.s.i	experiment [4]	DPM	DPM + f.s.i.
h^-	3.29	3.22 ± 0.06	95		98 ± 3	798	
π^-	3.06	3.06 ± 0.08	88		91 ± 3	742	
K^-	0.17	0.17 ± 0.05	7.0	7.4	6.9 ± 0.4	72	76.
K^+	0.24	0.24 ± 0.05	8.4	11.2 (10.6)	12.4 ± 0.4	80	127.5 (120.0)
K_0^s	0.20	0.20 ± 0.02	7.6	9.2 (8.9)	10.5 ± 1.7	75	101 (97.)
p	0.97	0.99 ± 0.15	24	19.5 (20.6)	—	194*	118 (130)
$\bar{p}$	0.05	0.05 ± 0.02	2.3	1.7	—	30	23
Λ	0.12	0.096 ± 0.010	3.7	9.3 (8.0)	9.4 ± 1	36	131 (116)
$\bar{\Lambda}$	0.014	0.013 ± 0.004	1.3	2.1	2.2 ± 0.4	18	27

Table 1

Table Caption

Average multiplicities of secondaries in NN, central SS collisions at 200 GeV/c per nucleon and central Pb-Pb at 160 GeV/c per nucleon, compared with available data. For nucleus-nucleus collisions the multiplicities of Λ, K^+ and K_0^s in DPM are also given before the final state interactions $\pi N \to K\Lambda$ and $\pi\bar{N} \to K\bar{\Lambda}$ are taken into account. The number of protons in Pb-Pb (followed by an asterix), corresponds to the combination $(p+n)/2$. The values of multiplicities within (without) a parenthesis correspond to the dashed (full) lines in Fig. 3. The nucleon multiplicities after final state interaction are obtained from the relation $n_{p(\bar{p})}^{DPM+f.s.i} = n_{p(\bar{p})}^{DPM} - \left(n_{\Lambda(\bar{\Lambda})}^{DPM+f.s.i} - n_{\Lambda(\bar{\Lambda})}^{DPM}\right) \times 1.6/2$ (see main text).

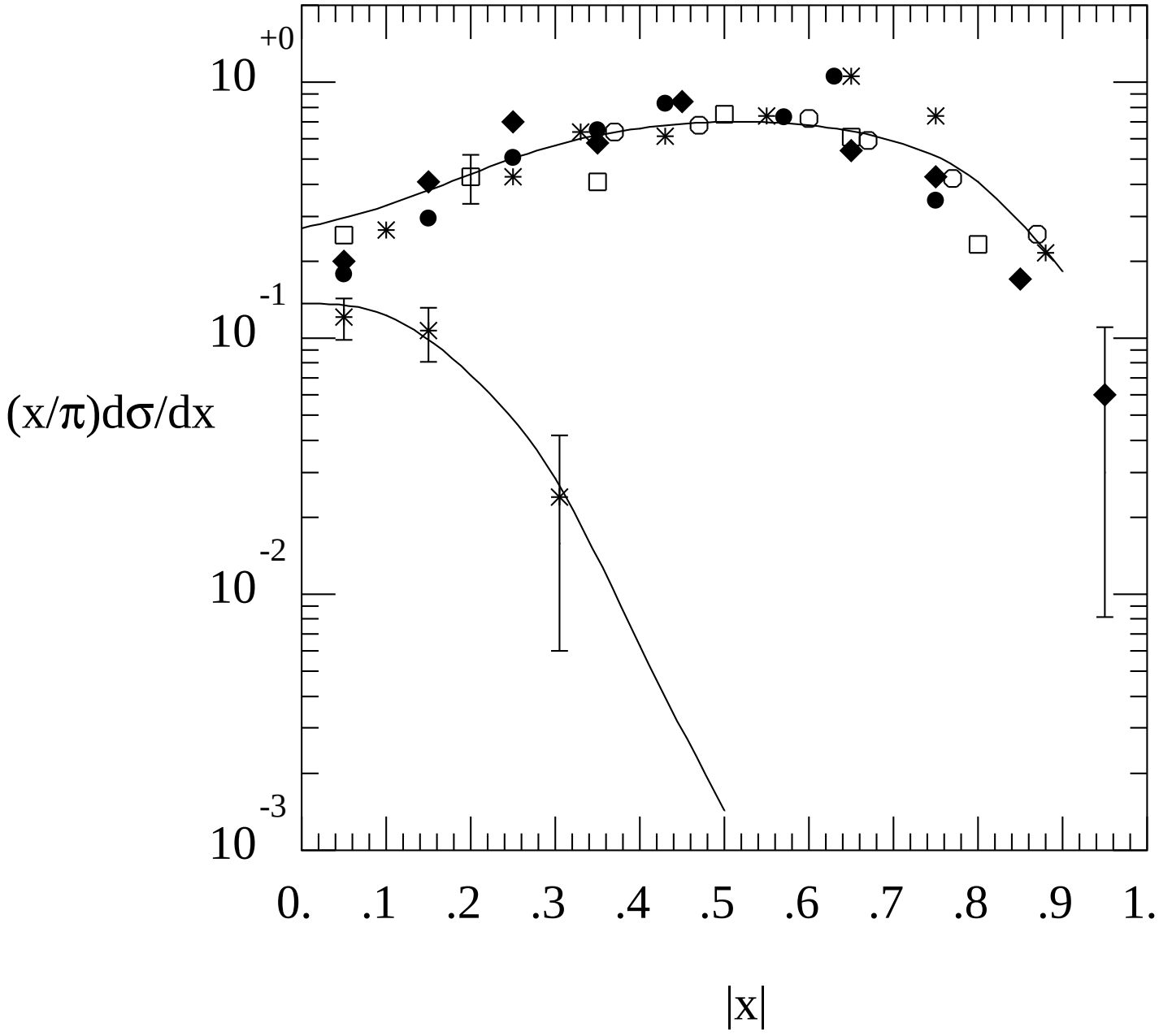

Fig. 1

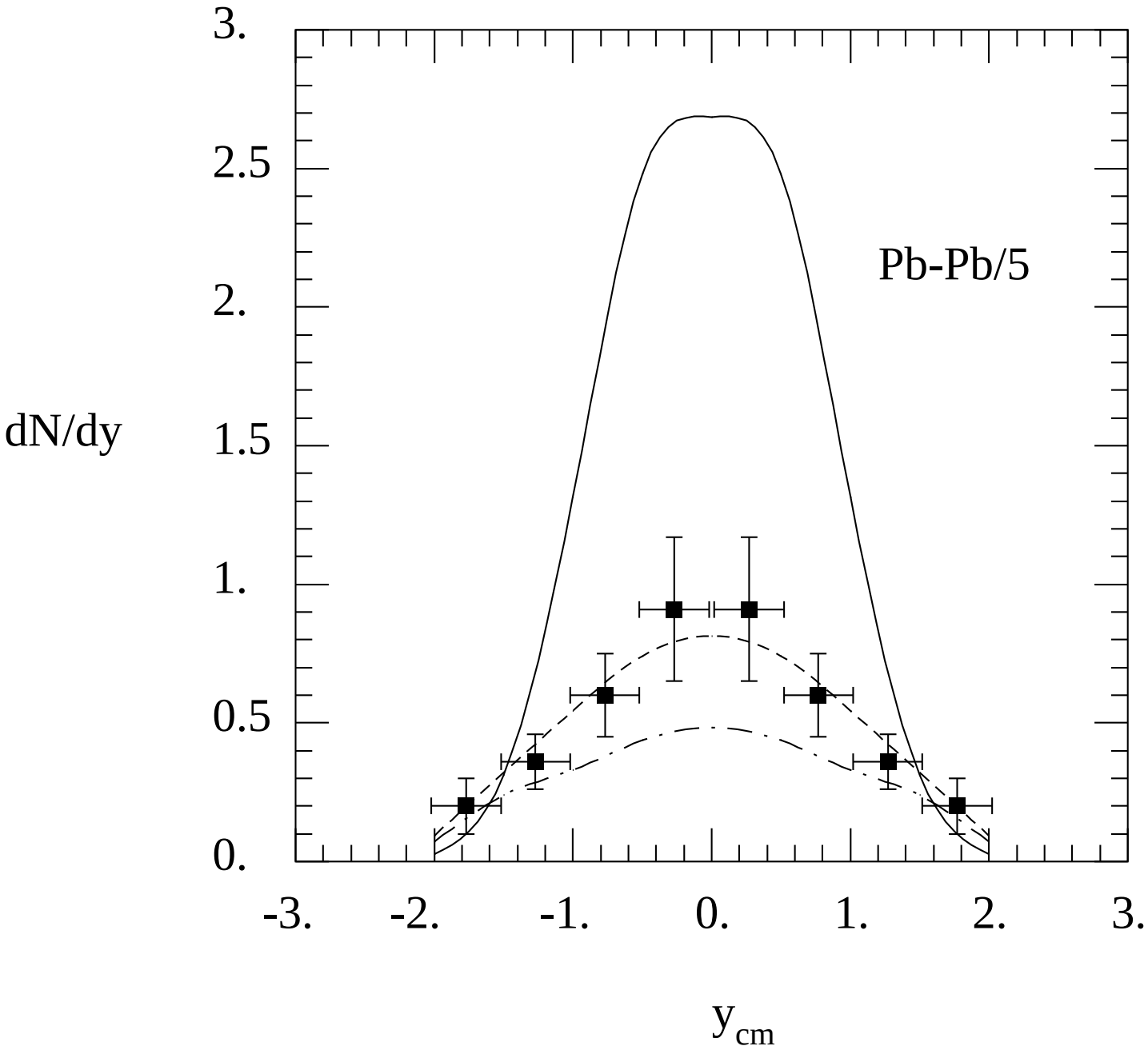

Fig. 2

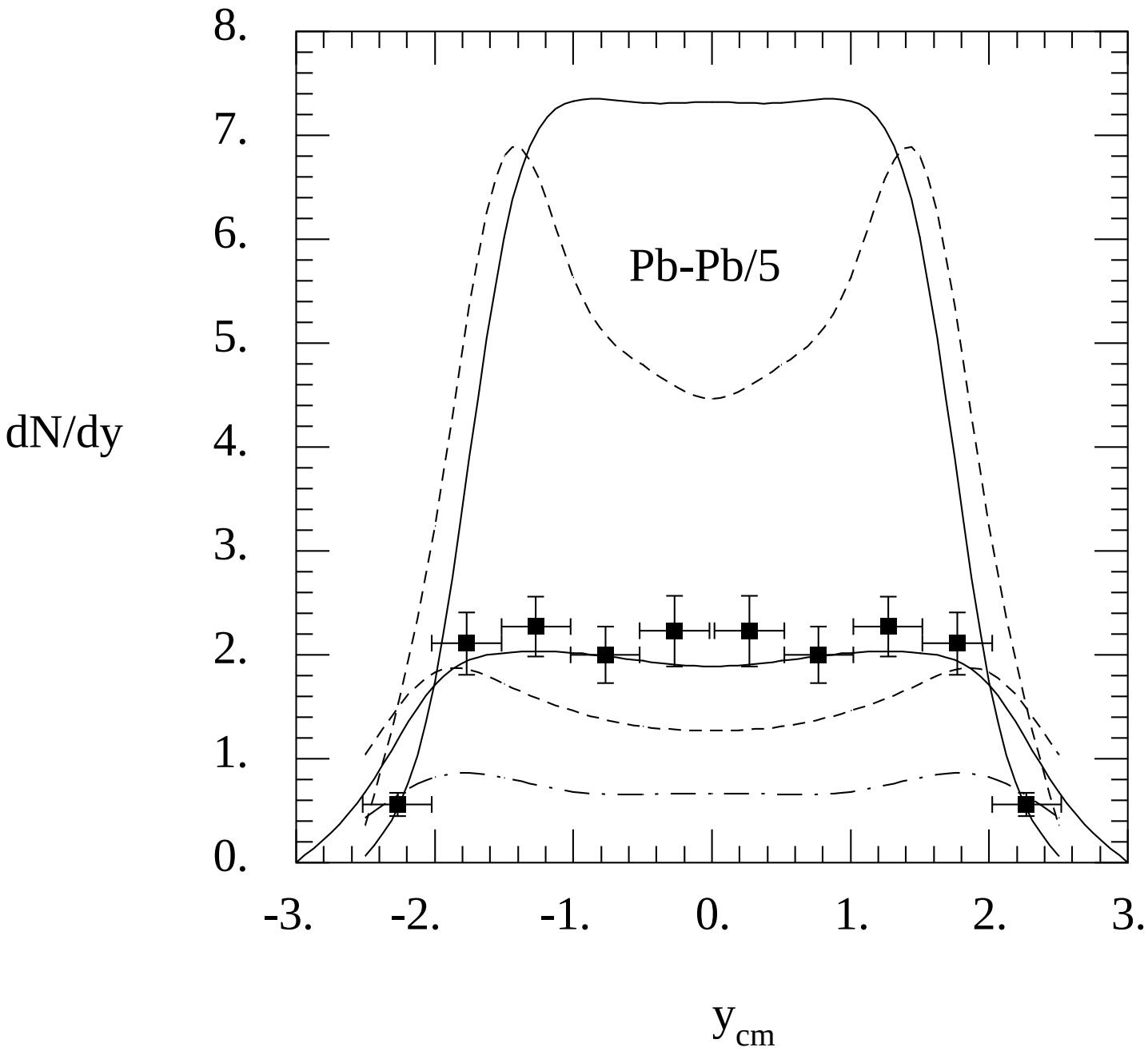

Fig. 3

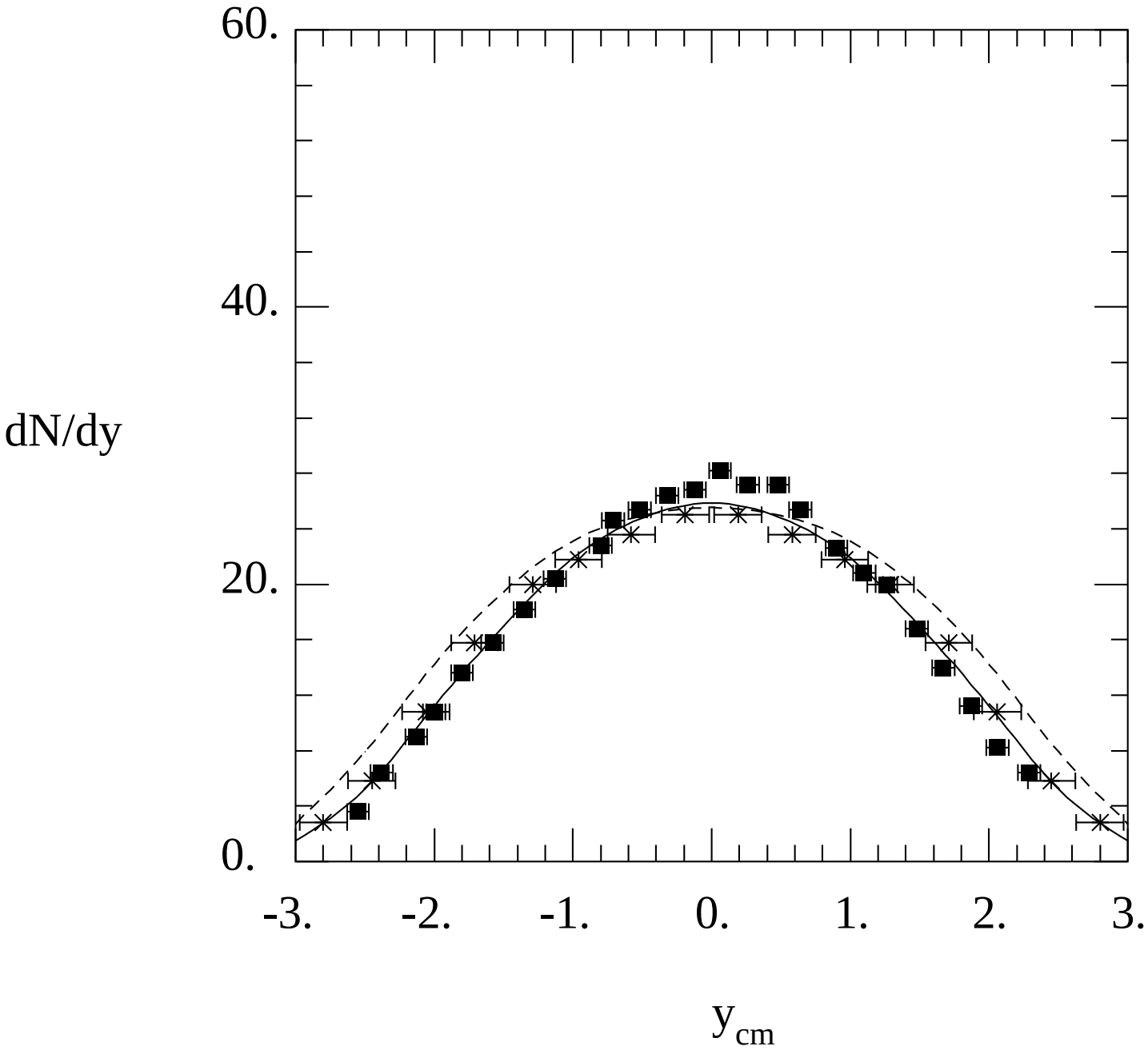

Fig. 4

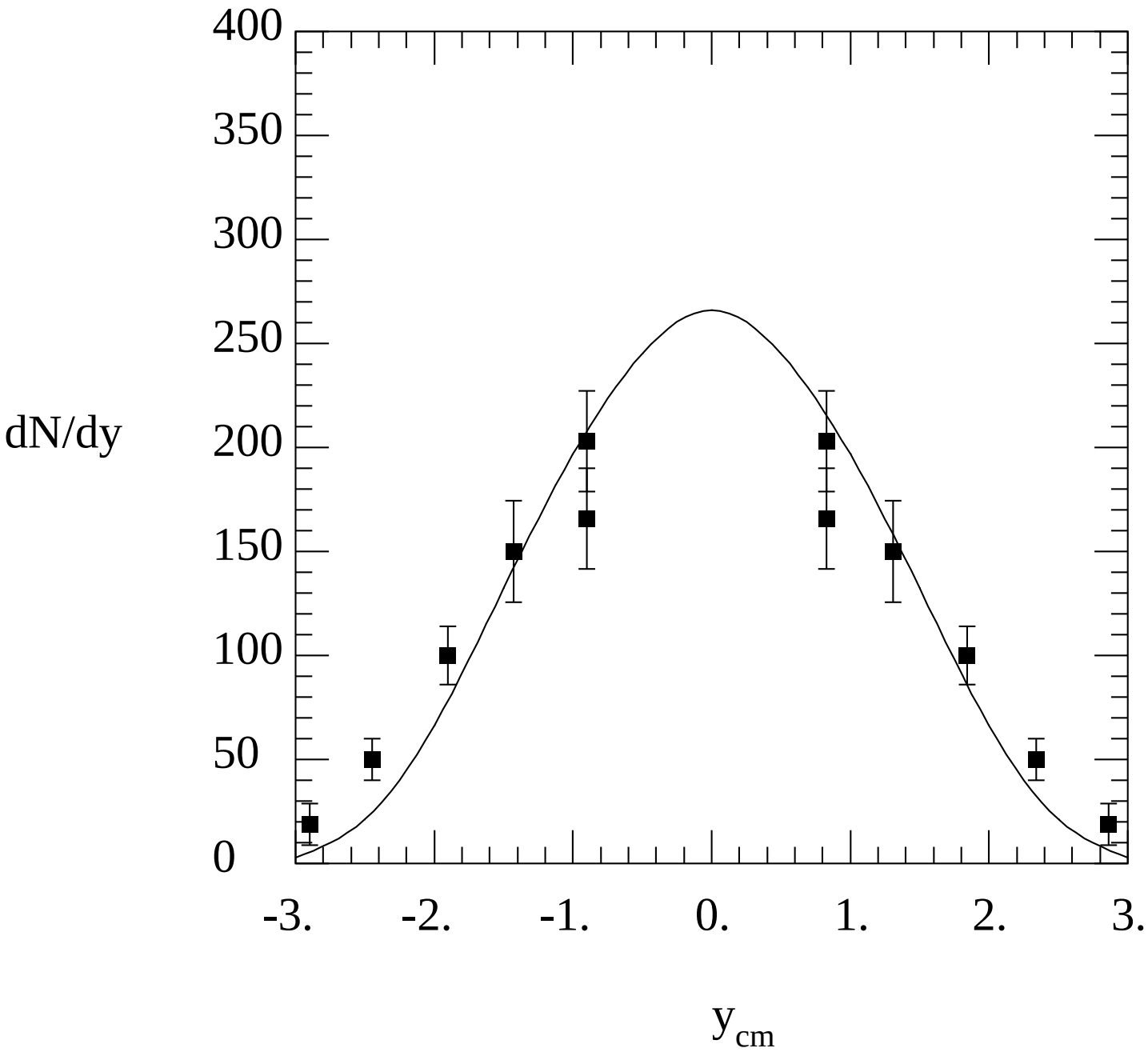

Fig. 5

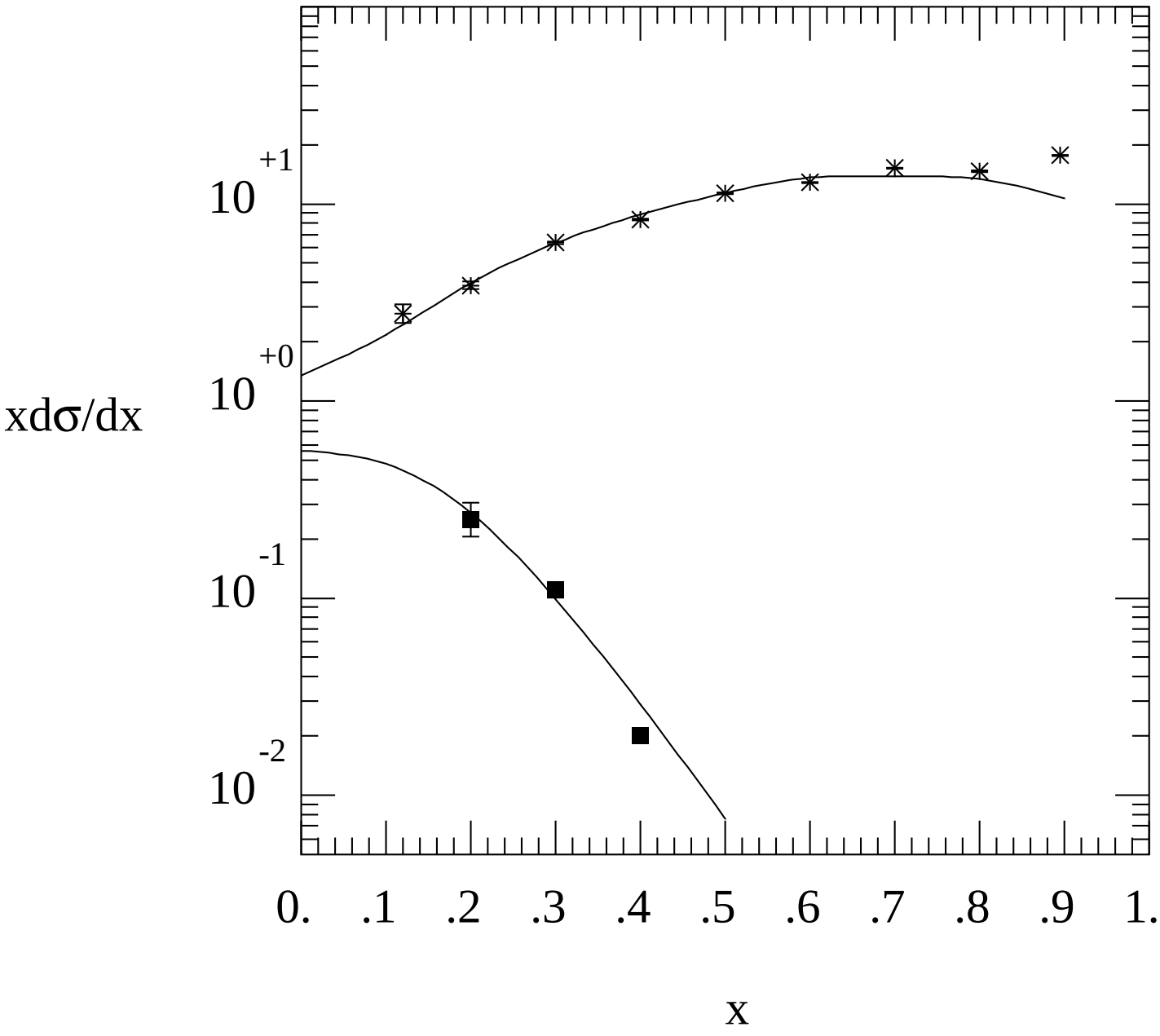

Fig. 6

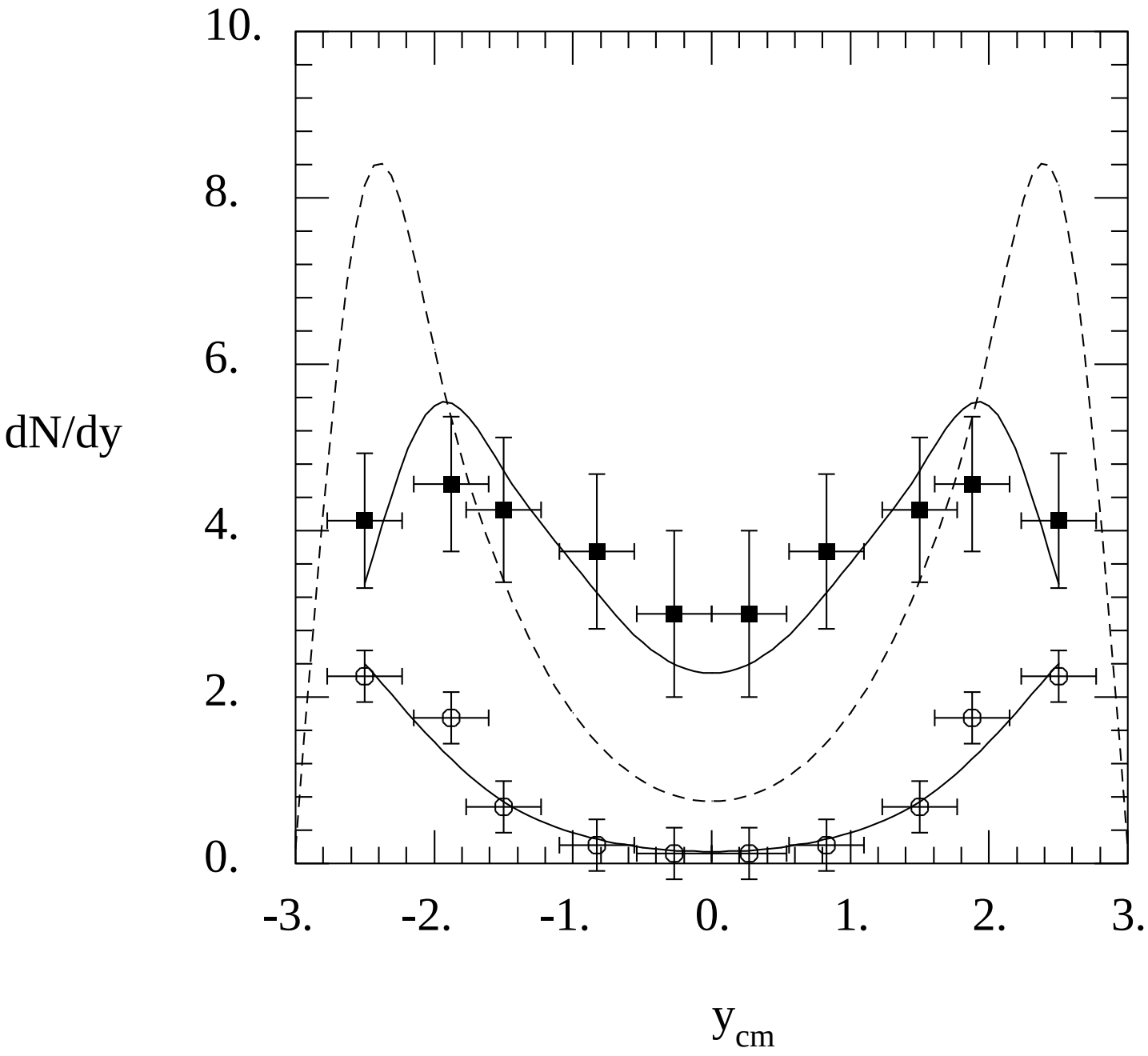

Fig. 7